NGC 5548 IN A LOW-LUMINOSITY STATE: IMPLICATIONS FOR THE BROAD-LINE REGION

Misty C. Bentz,[1] Kelly D. Denney,[1] Edward M. Cackett,[2,3] Matthias Dietrich,[1] Jeffrey K. J. Fogel,[3]
Himel Ghosh,[1] Keith D. Horne,[2] Charles Kuehn,[1,4] Takeo Minezaki,[5] Christopher A. Onken,[1,6]
Bradley M. Peterson,[1] Richard W. Pogge,[1] Vladimir I. Pronik,[7,8] Douglas O. Richstone,[3]
Sergey G. Sergeev,[7,8] Marianne Vestergaard,[9] Matthew G. Walker,[3] and Yuzuru Yoshii[5,10]

ABSTRACT

We describe results from a new ground-based monitoring campaign on NGC 5548, the best-studied reverberation-mapped AGN. We find that it was in the lowest luminosity state yet recorded during a monitoring program, namely $L_{5100} = 4.7 \times 10^{42}$ ergs s^{-1}. We determine a rest-frame time lag between flux variations in the continuum and the Hβ line of $6.3^{+2.6}_{-2.3}$ days. Combining our measurements with those of previous campaigns, we determine a weighted black hole mass of $M_{BH} = 6.54^{+0.26}_{-0.25} \times 10^7$ $M_{\odot}$ based on all broad emission lines with suitable variability data. We confirm the previously discovered virial relationship between the time lag of emission lines relative to the continuum and the width of the emission lines in NGC 5548, which is the expected signature of a gravity-dominated broad-line region. Using this lowest luminosity state, we extend the range of the relationship between the luminosity and the time lag in NGC 5548 and measure a slope that is consistent with $\alpha = 0.5$, the naive expectation for the broad-line region for an assumed form of $r \propto L^{\alpha}$. This value is also consistent with the slope recently determined by Bentz et al. for the population of reverberation-mapped AGNs as a whole.

Subject headings: galaxies: active — galaxies: nuclei — galaxies: Seyfert

1. INTRODUCTION

Reverberation mapping (Blandford & McKee 1982; Peterson 1993) is an extremely useful technique that has been exploited to measure the size of the broad-line region (BLR) for many nearby active galactic nuclei (AGNs). The time delay, or lag, between variations in the continuum flux and broad-line flux (usually Hβ) provides a measure of the size of the region from which the broad lines emanate. Coupling the measured lag time with the velocity width of the emission line provides an estimate of the mass of the central black hole. To date, 36 nearby Seyfert galaxies have BLR radius and black hole mass determinations from reverberation mapping (Peterson et al. 2004, 2005).

The Seyfert galaxy NGC 5548 was the focus of an intense, 13 yr campaign by the International AGN Watch consortium[11] (Peterson et al. 2002) to study the variations in the optical continuum and Hβ line flux. As a result, its emission line variability properties are well characterized.

During the spring of 2005, we undertook a new ground-based monitoring program (Bentz et al. 2006b; Denney et al. 2006) with the principal aim of replacing Hβ lag measurements and black hole mass estimates for several AGNs with previous, unsatisfactory data. We also monitored NGC 5548 and found that it was in the lowest luminosity state yet recorded during a monitoring campaign. In this paper, we present the low-luminosity monitoring data and combine it with previous monitoring results of NGC 5548 to examine several questions related to reverberation mapping and AGN variability. We explore the behavior of the BLR with respect to varying luminosity states in NGC 5548, and examine the intrinsic scatter in reverberation-based black hole mass measurements for a single object.

2. OBSERVATIONS AND DATA REDUCTION

2.1. *Spectroscopy*

For most of the clear nights between 2005 March 1 and April 10, we obtained spectra of the nucleus of NGC 5548, an S0/a Seyfert galaxy at $z = 0.01717$, with the Boller & Chivens CCD Spectrograph (CCDS) on the McGraw-Hill 1.3 m telescope at MDM Observatory. The observational details and data reduction are as described by Bentz et al. (2006b) but for completeness, we include a few of the details here. The observations of NGC 5548 were obtained at a position angle of $90°$ through a $5''$ slit, resulting in a spectral resolution of 7.6 Å over the wavelength range 4400–5650 Å. The typical seeing was $2''$.

Additional spectra were obtained at the Crimean Astrophysical Observatory (CrAO) 2.6 m Shajn Telescope with the Nasmith Spectrograph and Astro-550 580×520 pixel CCD (Berezin et al. 1991). The spectra were obtained through a $3''$ slit at a position angle of $90°$. Spectral reduction was carried out in the usual way with an extraction width of 16 pixels, corresponding to $11''$ on the sky.

[1] Department of Astronomy, The Ohio State University, Columbus, OH 43210; bentz@astronomy.ohio-state.edu, denney@astronomy.ohio-state.edu, dietrich@astronomy.ohio-state.edu, ghosh@astronomy.ohio-state.edu, peterson@astronomy.ohio-state.edu, pogge@astronomy.ohio-state.edu.

[2] School of Physics and Astronomy, University of St. Andrews, Fife, KY16 9SS, Scotland, UK; emc14@st-and.ac.uk, kdh1@st-and.ac.uk.

[3] Department of Astronomy, University of Michigan, Ann Arbor, MI 48109-1090; fogel@umich.edu, dor@umich.edu, mgwalker@umich.edu.

[4] Current address: Physics and Astronomy Department, Michigan State University, East Lansing, MI 48824; kuehncha@msu.edu.

[5] Institute of Astronomy, School of Science, University of Tokyo, 2-21-1 Osawa, Mitaka, Tokyo 181-0015, Japan; minezaki@mtk.ioa.s.u-tokyo.ac.jp, yoshii@mtk.ioa.s.u-tokyo.ac.jp.

[6] Current address: National Research Council Canada, Herzberg Institute of Astrophysics, 5071 West Saanich Road, Victoria, BC V9E 2E7, Canada; christopher.onken@nrc-cnrc.gc.ca.

[7] Crimean Astrophysical Observatory, p/o Nauchny, 98409 Crimea, Ukraine; sergeev@crao.crimea.ua, vpronik@crao.crimea.ua.

[8] Isaak Newton Institute of Chile, Crimean Branch, Ukraine.

[9] Steward Observatory, University of Arizona, Tucson, AZ 85721; mvestergaard@as.arizona.edu.

[10] Research Center for the Early Universe, School of Science, University of Tokyo, 7-3-1 Hongo, Bunkyo-ku, Tokyo 113-0033, Japan.

[11] See http://www.astronomy.ohio-state.edu/~agnwatch/.

<div style="text-align:center">

TABLE 1

CONTINUUM AND Hβ FLUXES FOR NGC 5548

</div>

JD[a] (−2,450,000)	F_λ (5100 Å) (10^{-15} ergs s^{-1} cm^{-2} Å^{-1})	Hβ λ4681 (10^{-13} ergs s^{-1} cm^{-2})	Observatory Code[b]
3431.996...............	6.15 ± 0.18	1.79 ± 0.05	M
3432.922...............	5.27 ± 0.52	...	H
3435.930...............	6.63 ± 0.39	...	H
3437.969...............	6.80 ± 0.20	...	H
3438.023...............	6.56 ± 0.19	2.04 ± 0.06	M
3438.922...............	6.74 ± 0.20	2.21 ± 0.07	M
3440.996...............	6.75 ± 0.20	2.19 ± 0.07	M
3441.980...............	6.64 ± 0.19	2.27 ± 0.07	M
3442.891...............	6.52 ± 0.30	...	H
3443.004...............	6.48 ± 0.19	2.26 ± 0.07	M
3443.996...............	6.52 ± 0.19	2.23 ± 0.07	M
3444.598...............	6.31 ± 0.30	2.30 ± 0.04	C
3445.594...............	6.13 ± 0.29	2.35 ± 0.04	C
3446.008...............	6.65 ± 0.19	2.29 ± 0.07	M
3447.000...............	6.45 ± 0.19	2.38 ± 0.07	M
3447.000...............	6.26 ± 0.17	...	H
3450.973...............	6.54 ± 0.19	2.26 ± 0.07	M
3451.922...............	6.68 ± 0.19	...	H
3451.941...............	6.51 ± 0.19	2.41 ± 0.07	M
3452.957...............	6.74 ± 0.20	2.22 ± 0.07	M
3456.949...............	7.08 ± 0.21	2.07 ± 0.06	M
3457.852...............	6.54 ± 0.67	...	H
3459.004...............	6.88 ± 0.20	2.48 ± 0.07	M
3459.922...............	6.87 ± 0.20	2.39 ± 0.07	M
3460.938...............	6.75 ± 0.20	2.51 ± 0.08	M
3461.887...............	7.25 ± 0.21	2.47 ± 0.07	M
3462.918...............	6.73 ± 0.20	2.46 ± 0.07	M
3463.527...............	6.99 ± 0.34	2.48 ± 0.04	C
3464.504...............	6.86 ± 0.33	2.45 ± 0.04	C
3464.891...............	6.69 ± 0.19	2.43 ± 0.07	M
3465.949...............	6.58 ± 0.19	2.51 ± 0.08	M
3466.070...............	7.04 ± 0.09	...	H
3466.922...............	7.33 ± 0.21	2.52 ± 0.08	M
3467.973...............	6.52 ± 0.19	2.50 ± 0.08	M
3468.957...............	6.45 ± 0.19	2.55 ± 0.08	M
3469.922...............	6.45 ± 0.19	2.42 ± 0.07	M
3470.012...............	6.49 ± 0.09	...	H
3470.926...............	6.53 ± 0.19	2.48 ± 0.07	M
3471.516...............	6.73 ± 0.32	2.31 ± 0.04	C
3471.922...............	6.34 ± 0.18	2.46 ± 0.07	M

[a] The Julian Date listed is the midpoint of the observation.
[b] Observatory Codes: C = CrAO 2.6 m Shajn Telescope + Nasmith Spectrograph; H = Haleakala Observatories 2.0 m MAGNUM Telescope + MIP; M = MDM Observatory 1.3 m McGraw-Hill Telescope + CCDS.

The spectra were then internally flux calibrated within each data set. We scaled each individual spectrum to an [O III] λ5007 flux of 5.58×10^{-13} ergs s^{-1} cm^{-2}; the flux of the [O III] λ5007 line determined by photometric spectra from the first year of the 13 yr ground-based monitoring program for NGC 5548 (Peterson et al. 1991), using the spectral scaling algorithm of van Groningen & Wanders (1992). This process minimizes the residuals of the [O III] λ5007 line in a difference spectrum by comparing individual spectra to a reference spectrum (in this case, the mean spectrum of all the data in the set) and scaling appropriately.

We then created light curves from measurements of the spectra. The mean continuum flux was measured between observed-frame wavelengths of 5170–5200 Å. The flux of the Hβ emission line was measured by first setting a linear continuum level between the observed-frame windows of 4800–4830 Å and 5170–
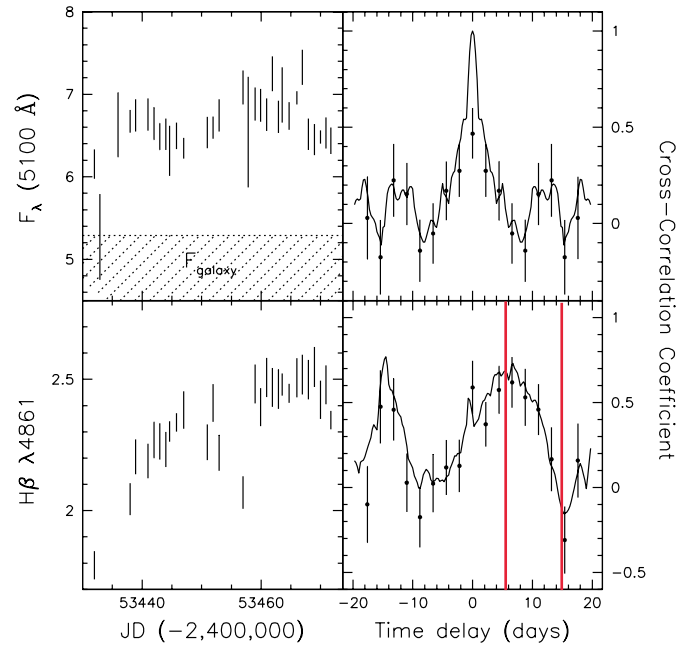

FIG. 1.—Left panels show the light curves for the continuum region at 5100 Å and for the Hβ λ4861 line. Measurements taken within a 0.5 day bin have been averaged together. The flux is in units of 10^{-15} ergs s^{-1} cm^{-2} Å^{-1} for the continuum and units of 10^{-13} ergs s^{-1} cm^{-2} for Hβ. The shaded area of the continuum light curve shows the contribution to the flux from the host galaxy. The right panels show the result of cross-correlating each light curve with the continuum light curve; the top right panel is therefore the continuum auto-correlation function. The solid line shows the ICCF method, while the points show the DCF method, as described in the text.

5200 Å, and then integrating the flux above the best-fit continuum between 4850–5000 Å in the observed frame.

2.2. Photometry

Photometry in the V band was obtained at the 2.0 m Multicolor Active Galactic Nuclei Monitoring (MAGNUM) telescope at the Haleakala Observatories in Hawaii (Kobayashi et al. 1998b; Yoshii 2002; Yoshii et al. 2003) with the multicolor imaging photometer (MIP; Kobayashi et al. 1998a). Following the procedure explained by Suganuma et al. (2004), the nuclear flux of NGC 5548 was measured relative to a nearby reference star located at $(\Delta\alpha, \Delta\delta) = (-0.1', -2.6')$. After processing the frames in the usual way with IRAF, aperture photometry was performed within an aperture radius of 4.15″, with sky subtraction between radii of 5.5″–6.9″. The reference star was then calibrated using photometric standard stars from Landolt (1992) and Hunt et al. (1998). Variability of the reference star was previously shown to be negligible by Suganuma et al. (2004). Due to technical issues with the instrument, the photometric accuracy was very low at the beginning of this monitoring campaign, but improved considerably toward the end when the instrument was fixed (note the magnitude of the uncertainties listed in Table 1 and the size of the error bars in Fig. 1).

2.3. Intercalibration of Light Curves

As a result of the varying slit geometries, extraction apertures, and seeing conditions in each of the spectroscopic and imaging data sets, they must be intercalibrated with each other to account for slit losses and different amounts of host galaxy starlight flux. We follow the process described by Bentz et al. (2006b) to scale the CrAO and MAGNUM data sets to the MDM data set by

TABLE 2
Light Curve Statistics

Time Series (1)	N (2)	Sampling Interval (days)		Mean Flux[a] (5)	Mean Fractional Error (6)	F_{var} (7)	R_{max} (8)
		$\langle T \rangle$ (3)	T_{median} (4)				
5100 Å	31	1.3	1.0	6.63 ± 0.36	0.033	0.040	1.39 ± 0.14
Hβ	28	1.5	1.0	2.34 ± 0.17	0.027	0.069	1.42 ± 0.06

[a] Fluxes are in the same units as those used in Table 1.

using a least-squares analysis to identify the flux offsets relative to the MDM data set. After correcting for these offsets, the three data sets were merged into a continuum light curve and Hβ light curve, which are tabulated in Table 1. For the analysis that follows, we combined observations within a 0.5 days window, which yields the final light curves that are depicted in Figure 1. The points with the large error bars are those from the MAGNUM telescope while the instrument was experiencing difficulties.

Table 2 describes the statistical properties of the final continuum and emission-line light curves. Column (1) lists the spectral feature of the timeseries and column (2) gives the number of measurements. The mean and median sampling interval between data points are given in columns (3) and (4), respectively. The mean flux and standard deviation of the timeseries are given in column (5). The continuum flux measurement does not take into account the host galaxy starlight contribution. Using a high-resolution *Hubble Space Telescope* image of NGC 5548 and the procedures described by Bentz et al. (2006a) we measure the host galaxy contribution through the larger slit geometry in this study ($5.0'' \times 12.75''$) to be $F_{gal}(5100 \text{ Å}) = (5.29 \pm 0.49) \times 10^{-15}$ ergs s^{-1} cm^{-2} Å^{-1}. The mean fractional error, which is based on closely spaced observations in time, is given in column (6). Column (7) is the excess variance, which is computed as

$$F_{var} = \frac{\sqrt{\sigma^2 - \delta^2}}{\langle f \rangle}, \qquad (1)$$

where σ^2 is the variance of the fluxes, δ^2 is their mean-square uncertainty, and $\langle f \rangle$ is the mean of the observed fluxes. Lastly, column (8) is the ratio of the maximum to the minimum flux in each timeseries. Comparison of the values of F_{var} for the continuum and Hβ fluxes with those determined for the previous 13 years of monitoring data show that the amplitude of variation in the continuum is about half that of the previous lowest continuum-variability year (Year 7 [1995] of Peterson et al. 2002), and the amplitude of variability in the Hβ line is the third lowest measured (see also Year 5 [1993] and Year 11 [1999] of Peterson et al.).

Correcting the mean optical flux for the host galaxy contribution above, we find that NGC 5548 was in the lowest luminosity state yet recorded during a monitoring campaign, only $F_{AGN}(5100 \text{ Å}) = (1.3 \pm 0.5) \times 10^{-15}$ ergs s^{-1} cm^{-2} Å^{-1}. This is a full 40% fainter than the previous record holder, Year 4 (1992) of the AGN Watch campaign (see Peterson et al. 2002 for the original flux measurement and Bentz et al. 2006a for the host galaxy correction).

3. DATA ANALYSIS

3.1. *Time Series*

As a result of the low luminosity of the AGN and the very low level of variability throughout the campaign, it is quite evident that determining a time lag can be problematic. However, we proceed with the usual tools developed for reverberation map-

ping to see whether a statistically significant detection can still be culled from the data. To measure the time lag between the continuum and the broad part of the Hβ emission line, we employ the interpolation cross-correlation function (ICCF) method of Gaskell & Sparke (1986) and Gaskell & Peterson (1987) and the discrete correlation function (DCF) method of Edelson & Krolik (1988), with the modifications discussed by White & Peterson (1994) in both cases. To quantify the uncertainties in the time delay measurement, we follow the method described by Bentz et al. (2006b) originally outlined by Peterson et al. (1998) with the modifications of Peterson et al. (2002). Figure 1 shows the continuum and emission-line light curves and cross-correlation results.

For the light curves of NGC 5548 shown in Figure 1, we find the cross-correlation centroid occurs at $\tau_{cent} = 6.4^{+2.6}_{-2.3}$ days and the peak of the cross-correlation function (for physical lag times $\tau > 0$) occurs at $\tau_{peak} = 6.5^{+2.5}_{-2.5}$ days in the observed frame. Following the consideration of the relative merits of τ_{cent} versus τ_{peak} by Peterson et al. (2004), we will use the value of τ_{cent} corrected for time dilation effects by a factor of $(1 + z)$, $\tau_{cent} = 6.3^{+2.6}_{-2.3}$ days, in the discussion that follows.

A measure of the quality of the data can be estimated by analysis of the auto-correlation function of the continuum in the top right panel of Figure 1. The ICCF and DCF methods give very different values at $\tau = 0$, the peak of the ICCF is 1.0, compared with the peak of the DCF, $\sim$0.5. This discrepancy arises from the fact that we have discarded measurements of the DCF where τ is exactly equal to 0 (i.e., simultaneous pairs measured from the same spectrum) because they are subject to correlated errors, especially when the amplitude of variability is so low. The DCF with zero-lag pairs excluded therefore gives a more realistic measure of the correlation of nearby data points with each other because, unlike the ICCF, it does not include correlation of the noise in the data with itself. With such noisy data and low-level signals in the light curves, it is rather remarkable that we are able to obtain a statistically significant time lag between the continuum and Hβ light curves.

To further quantify the significance of this detection, we have carried out the following Monte Carlo simulations. An optical continuum light curve was generated using the characteristics of the power density spectrum measured for NGC 5548, $P(f) \propto f^{-2.56}$ (Collier & Peterson 2001). The model continuum light curve was then convolved with a transfer function to produce a model emission-line light curve. Two simple models for the transfer function were employed for illustrative purposes:

1. A thin, spherical shell of radius $R = 6.3$ light days, which has a constant response from $\tau = 0$ to $\tau = 2R/c$ and is zero everywhere else. Such a transfer function results in the most smoothing of the continuum light curve shape as it is transferred to the line light curve.

2. A thin disk of radius $R = 6.3$ light days and inclination $0°$, which is a delta function at $\tau = R/c$. This transfer function results
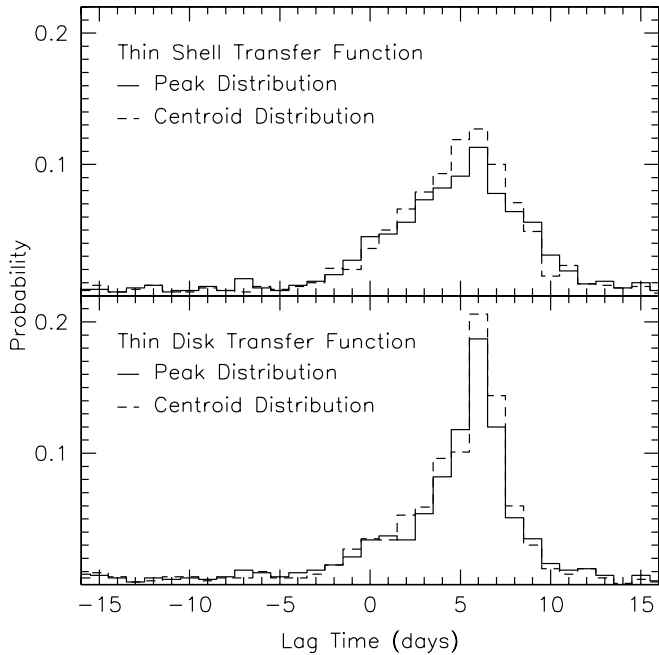
Fig. 2.—Cross-correlation peak distributions (*solid lines*) and centroid distributions (*dashed lines*) for the Monte Carlo simulations described in the text. The top panel is for a thin-shell transfer function, and the bottom panel is for a thin-disk transfer function.

in the sharpest transfer of structural features from the continuum light curve to the emission-line light curve.

For ideal data, each of these cases would yield a lag measurement of $\tau = R/c$.

After creating the model light curves, they were sampled in the same pattern as the observations presented in this paper. The sampled points were rescaled according to the excess variances and mean fractional errors determined for the real data set and presented in Table 2. To simulate noise, each data point was randomly altered by a Gaussian deviate within the flux uncertainties appropriate for the observing campaign. The simulated set of observations was then cross-correlated in the manner described above, and the peak and centroid of the cross correlation was recorded. This entire process, beginning with the model continuum generation, was repeated 1000 times for each of the transfer functions described above. The resulting cross-correlation peak and centroid distributions for the two transfer functions are displayed in Figure 2. Casual inspection of the distributions in Figure 2 shows that most of the simulation results pile up around the expected lag measurement of 6.3 days, which lends much confidence to the measurements made above for our observing campaign.

About 15% of the simulations result in unphysical lag times, that is, $\tau < 0$, indicating that the broad-line flux responds before the continuum flux varies. Considering only those simulations that have physically plausible lag times ($\tau \geq 0$), we find that for the thin-shell transfer function, 53% of the peak measurements and 56% of the disk measurements fall within the range of 1 σ uncertainties quoted above for the lag measured in our observing campaign. The percentages increase to 69% and 67%, respectively, for the thin-disk transfer function. The asymmetric shapes of the peak and centroid distributions result in slightly lower median lag times than expected; however, the medians are well within 1 σ of the input lag time of 6.3 days: $\tau_{peak} = 5.8^{+3.0}_{-3.2}$ and

$\tau_{cent} = 5.5^{+2.8}_{-3.0}$, based on the simulations with a thin-shell transfer function, and $\tau_{peak} = 6.0^{+1.8}_{-2.5}$ and $\tau_{cent} = 5.8^{+1.7}_{-2.8}$, based on the simulations with a thin-disk transfer function. The fact that the thin-disk model seems to more accurately reproduce the observed data is not surprising: Horne et al.(1991) find strong evidence ruling out a spherically symmetric geometry for the Hβ BLR of NGC 5548. The most likely geometry is probably somewhere in between these two simple models; however, the models are useful in that they approximate the two opposite extremes of possible BLR behavior in AGNs in the sense of minimal (face-on disk) versus maximal (spherical shell) smoothing of the line light curve shape. In any case, the simulations clearly confirm the detected rest-frame lag of 6.3 days.

3.2. *Line Width Measurement*

The mean and root mean square (rms; i.e., variable) spectra of NGC 5548 were calculated using the full set of MDM data and are shown in Figure 3. To measure the width of the broad emission line, we first subtract the [O III] $\lambda4959$ narrow line using the [O III] $\lambda5007$ emission line as a template and the standard scaling factor of 0.340 for the $\lambda4959$ line relative to the $\lambda5007$ line (Storey & Zeippen 2000). We also subtract the narrow component of the Hβ line using the same template and the scaling value of 0.110 for the ratio of the lines determined by Peterson et al. (2002). We then interpolate the continuum underneath the broad Hβ emission line by setting continuum windows on either side of the line. The width of the line is typically characterized by its full width at half maximum (FWHM) and by the second moment of the line profile, the line dispersion (σ_{line}), as described by Peterson et al. (2004) and is corrected for the spectral resolution. In this case, since the red side of the mean profile can be contaminated by Fe II multiplet 42 emission and artifacts of the [O III] removal, we also include in our line measurements the line dispersion based on the blue side of the line, assuming the profile is approximately symmetric around the expected central wavelength of the line, which we denote $\sigma_{blue,sym}$. The uncertainties in the line width measurements are determined using the method described by Bentz et al. (2006b); however, the formal uncertainties for the σ_{line} and $\sigma_{blue,sym}$ measurements in the mean spectrum of 0.6% are probably misleading since the measurement errors are mostly systematic in this low state of variability. We therefore adopt an error of 20%, which is more typical of the errors in mean profile widths.

Table 3 lists the line widths measured for NGC 5548 in the mean spectrum, where the signal is much stronger, as well as the rms spectrum. For this particular data set, the FWHM of the variable (rms) broad line is not well characterized, so we omit this measurement. Fortunately, all measurements of the line width tabulated in Table 3 are consistent with each other even though the rms spectrum in particular has an extremely low-level signal. While the line width measurement that is typically preferred for reverberation-mapping data sets is σ_{line}(rms) (Collin et al. 2006), due to the low-level signal in the rms spectrum, we will choose to use a measurement from the mean spectrum in this case. The blending problems between the red side of the Hβ line and the [O III] $\lambda4959$ line and other features cause us to adopt $\sigma_{blue,sym}$ (mean) as the most credible line width for this data set in the following discussion. While we have noted that all the line width measurements for this data set are consistent with each other, so the choice of line width does not have a critical impact on the following discussion, there are issues that effect certain measurements and not others, so a combination of the line width measurements is not appropriate here.
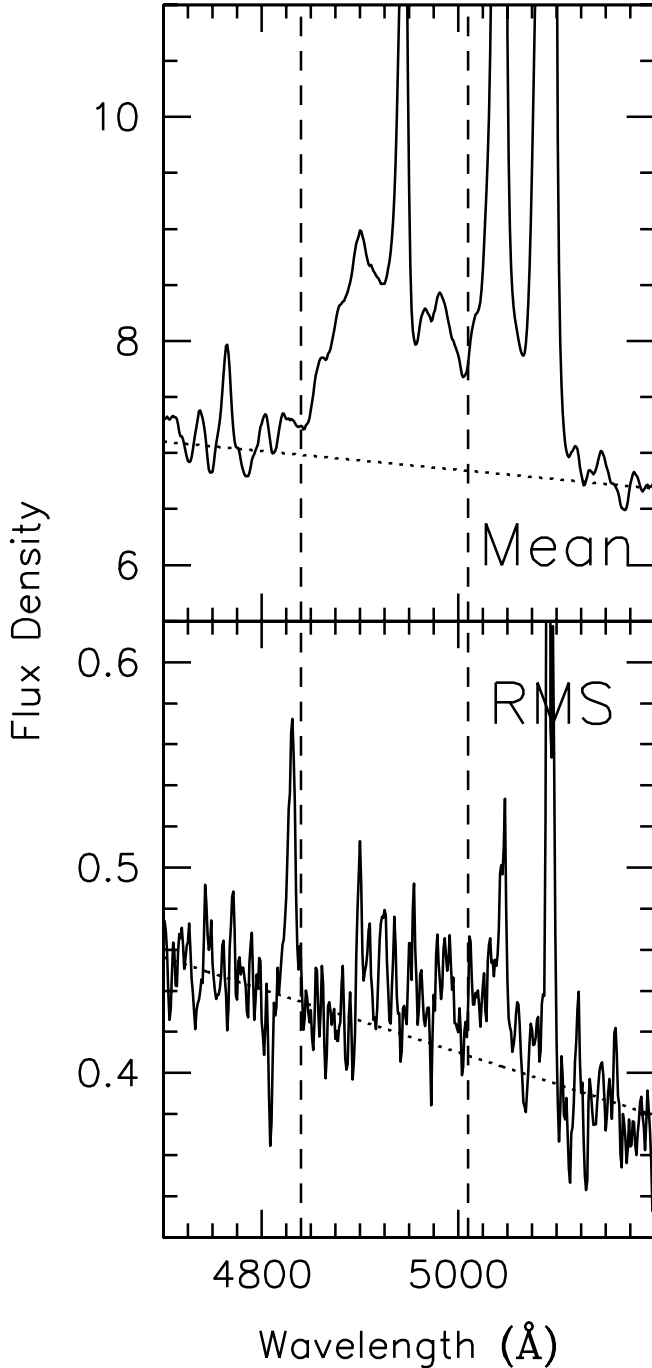
TABLE 3
Hβ LINE WIDTH MEASUREMENTS

Line Width Measurement	Mean Spectrum (km s^{-1})	rms Spectrum (km s^{-1})
σ_{line}	2662 ± 532	2388 ± 373
$\sigma_{blue,sym}$	3210 ± 642[a]	2939 ± 768
FWHM	6396 ± 167	. . .

[a] The preferred measurement of the width of Hβ for the new data presented in this paper.

tional constant. The factor f takes into account the unknown inclination, geometry, and kinematics of the BLR. Onken et al. (2004) have found that an average value $\langle f \rangle = 5.5 \pm 1.7$ if the relationship between black hole mass and stellar velocity dispersion (M_{BH}-σ_*) for AGNs is normalized to that of quiescent galaxies. With this normalization, we find $M_{BH} = 7.0^{+4.0}_{-3.7} \times 10^7 \ M_\odot$. Combining this new measurement with all previous reverberation-based mass measurements of the black hole in NGC 5548, we find a weighted mean of $M_{BH} = 6.83^{+0.30}_{-0.28} \times 10^7 \ M_\odot$ based on Hβ measurements only, and $M_{BH} = 6.54^{+0.26}_{-0.25} \times 10^7 \ M_\odot$ when including all measurements of broad lines. The reverberation-based mass is in good agreement with the mass expected from the M_{BH}-σ_* relationship of Tremaine et al. (2002), which predicts $M_{BH} = 9.4^{+7.6}_{-4.2} \times 10^7 \ M_\odot$ based on the stellar velocity dispersion measurement for NGC 5548 of $\sigma_* = 183 \pm 27$ km s^{-1} (Ferrarese et al. 2001). Considering the low-level signals of both the time lag and the line width in this low-luminosity data set, it is rather remarkable that our results are consistent with the expectations based on previous monitoring programs, as well as other methods of estimating the black hole mass for NGC 5548.

4. DISCUSSION

With the addition of this lowest luminosity data set to the compilation of NGC 5548 monitoring data, we examine several relationships between luminosity and other parameters where this experiment extends the range that may be explored.

4.1. Relationship between Line Width and Time Lag

Figure 4 shows the width of broad emission lines (σ_{line}) measured in NGC 5548 versus their time lag relative to the continuum at 5100 Å (τ_{cent}). If the BLR kinematics are dominated by gravity, we expect that there will exist a virial relationship between the time lag and the width of an emission line. The top panel shows the relationship for only those measurements of the Hβ line in NGC 5548, and the bottom panel includes all broad lines available. In either case, the slope is basically the same, about -0.5 ± 0.1, consistent with the virial relationship previously reported for NGC 5548 (Peterson & Wandel 1999; Peterson et al. 2004).

4.2. Relationship between Time Lag and Luminosity

Photoionization models of the BLR are typically parameterized by the shape of the ionizing continuum incident on the BLR gas, and an ionization parameter U, defined as

$$U = \frac{Q(H)}{4\pi r^2 n_H c}, \qquad (3)$$

where $Q(H)$ is the number of ionizing photons emitted from the continuum source per second, r is the size of the BLR, and n_H is the BLR particle density. We would naively expect that as the ionizing continuum luminosity varies, each emission line should

FIG. 3.—Mean and rms of the MDM spectra in the observed frame of NGC 5548. The rms spectrum still shows contributions from the [O III] λ4959 and λ5007 lines due to imperfect subtraction of all the nightly line profiles. The spike at 4825 Å appears to be due to a bad column in the detector. The dashed lines in both windows show the wavelength limits, and the dotted lines show the continuum levels used in calculating the width of the broad Hβ line. The flux density for both spectra is in units of 10^{-15} ergs s^{-1} cm^{-2} Å^{-1}.

3.3. Black Hole Mass

The mass of the central black hole is determined by

$$M_{BH} = \frac{fc\tau \Delta V^2}{G}, \qquad (2)$$

where τ is the time delay of the emission line, ΔV is the width of the emission line, c is the speed of light, and G is the gravita-
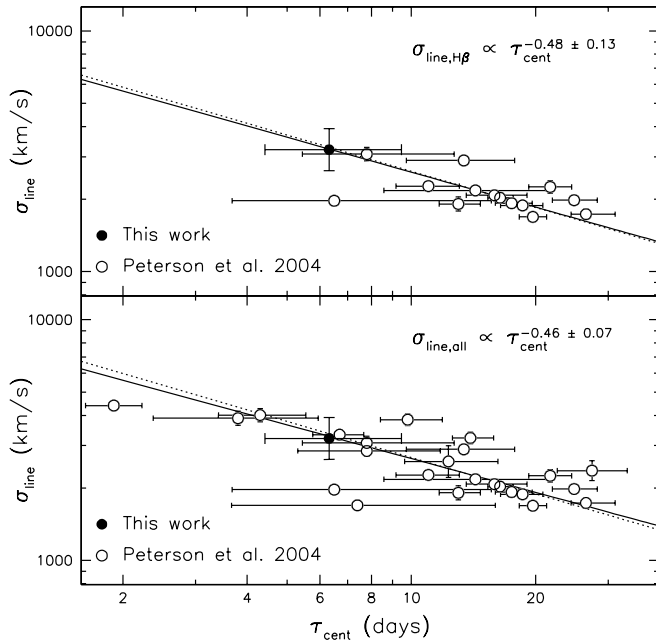
FIG. 4.—Rest-frame emission-line widths vs. time lags for NGC 5548. The top box shows the relationship for all measurements of the Hβ line, while the bottom box shows the relationship for measurements of all lines. The filled circles show the measurement of Hβ from this work, while the open circles are from Peterson et al. (2004). The solid lines are the best fits to the data, and the dotted lines are fits with a forced slope of -0.5, i.e., a virial relationship.

have the greatest response at some particular value of $Un_{\rm H}$. This would then lead to the expectation that, for any given line, $r \propto L_{\rm ion}^{1/2}$.

In Figure 5 we plot the relationship between the Hβ time lag relative to the continuum and the luminosity of the AGN at 5100 Å. If we include all 13 years of data from the AGN Watch campaign and the new low-luminosity data supplied in this work, we find a power-law slope of 0.73 ± 0.14. However, the data from Year 12 (2000) of the AGN Watch program is the most poorly sampled of all the monitoring campaigns for NGC 5548. The cross-correlations of the Hβ emission line with the continuum in the Year 12 data yields very ambiguous results, as can easily be seen in Figure 2 of Peterson et al. (2002). If we remove the Year 12 data point based on its potential unreliability, we find a power-law slope of 0.66 ± 0.13, within $\sim 1~\sigma$ of the naive expectation of 0.5. Using this relationship and the mean luminosity of NGC 5548, we estimate that the lag time for the Year 12 campaign should have been measured at ~ 11 days rather than $\tau_{\rm cent} = 6.6^{+5.8}_{-3.8}$ days as determined by Peterson et al. (2004). With the large error bars due to the ambiguous results of the cross-correlations for Year 12, the expected value of 11 days is within 1 σ of the measured value of 6.6 days. Based on these arguments, we are more inclined to accept the slope of 0.66 ± 0.13.

One would expect that a measurement of the AGN luminosity in the ultraviolet (UV) would give a much better estimate of $L_{\rm ion}$ than in the optical part of the spectrum. In Figure 6, we examine the relationship between 83 pairs of optical flux measurements at 5100 Å, $F_{\rm opt}$ (5100 Å), and UV flux measurements at 1350 Å, $F_{\rm UV}$ (1350 Å), for NGC 5548. The UV and optical flux measurements in each pair were made within 1 day of each other, and no statistically significant time delay exists between the optical and UV data (see Peterson et al. 2002 for a discussion of the data). The optical fluxes have been corrected using the host galaxy starlight contribution measured by Bentz et al. (2006a). The best power-law fit to the data is $F_{\rm opt} \propto F_{\rm UV}^{0.84 \pm 0.05}$. If we combine this
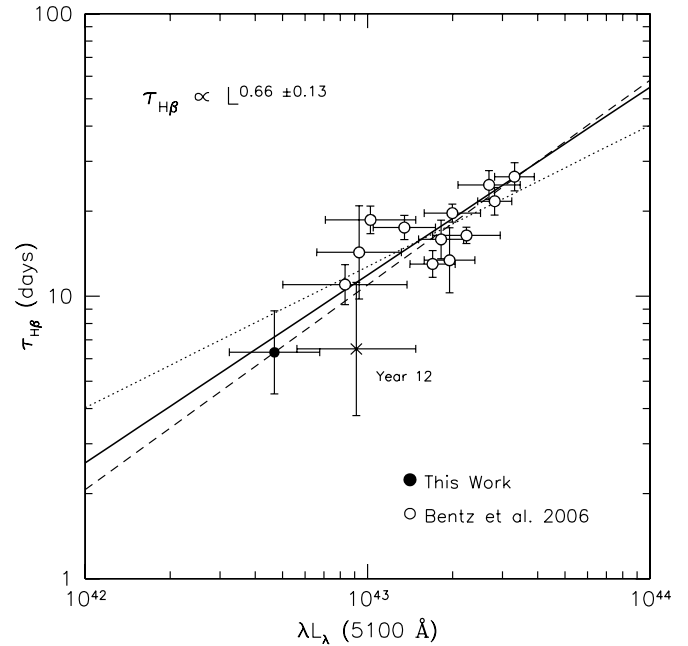

FIG. 5.—Rest-frame Hβ time lag vs. the luminosity at 5100 Å. The open circles are from Bentz et al. (2006a) after the luminosity measurement has been corrected for the host galaxy starlight contribution, and the filled circle is from this work, also corrected for host galaxy starlight. The dashed line has a slope of 0.73 ± 0.14 and shows the fit to the data with all the points included. The solid line shows the fit excluding the data from Year 12, with a slope of 0.66 ± 0.13, which we take to be the best current fit to the data for NGC 5548. The dotted line has a forced slope of 0.5, as one would expect from naive predictions of the behavior of the gas in the BLR to changes in the ionizing flux.

with the above r-$L_{\rm opt}$ fit excluding the data from Year 12, we find $r \propto L_{\rm UV}^{0.55 \pm 0.14}$. Interestingly, this is consistent not only with the naive expectation of how an object should behave when it varies over time, but also with the relationship recently determined by Bentz et al. (2006a) for the population of reverberation-mapped
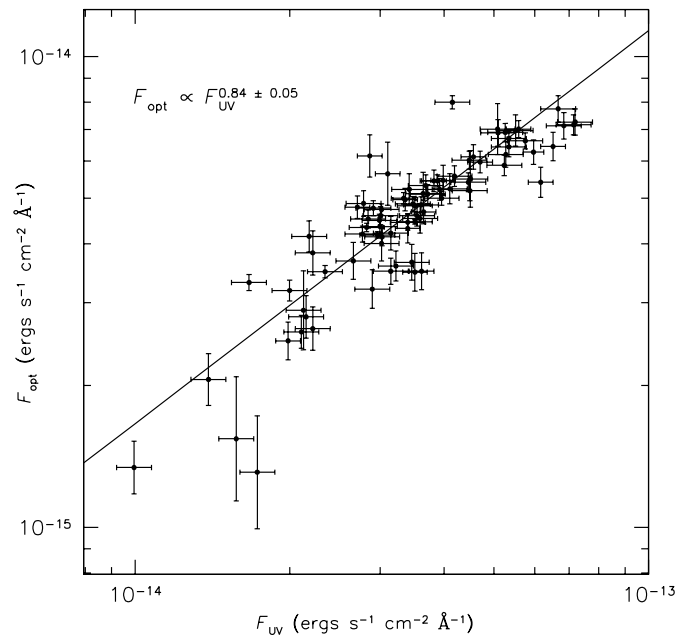

FIG. 6.—Optical flux at 5100 Å, after correction for host galaxy starlight, vs. the ultraviolet flux at 1350 Å. Each pair of optical and UV measurements was made within one day. The solid line shows the best fit, which has a power-law slope of 0.84 ± 0.05.
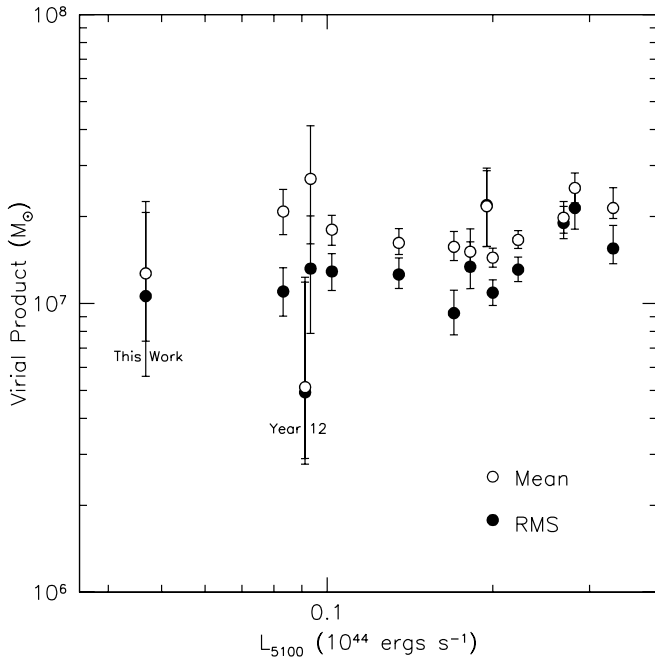
Fig. 7.—Virial product determined with σ_{line} calculated from the mean spectrum (*open circles*) and the rms spectrum (*filled circles*) vs. the luminosity at 5100 Å after correction for the contribution from host galaxy starlight.

AGNs as a whole. On the other hand, Cackett & Horne (2006) find a much shallower slope when modeling the 13 years of AGN Watch data for NGC 5548 as one continuous light curve with a luminosity-dependent delay map, more in agreement with the predictions of detailed photoionization models by Korista & Goad (2004). However, Cackett & Horne used a smaller correction for the host galaxy starlight contribution to the flux, which would serve to artificially flatten the relationship they find.

4.3. *Black Hole Mass Estimates*

The most obvious relationship left to examine is whether the black hole mass determinations are changing with the luminosity of the AGN. We expect that this would not be the case, as the black hole mass should not be changing in a measurable way and it certainly should not depend on the luminosity. Figure 7 shows the distribution of virial products (the black hole mass without the average scaling factor of 5.5, i.e., M_{BH}/f) as a function of luminosity. This is similar to the recent analysis by Collin et al. (2006) in that the open circles are those based on the measurement of $\sigma_{blue,sym}$ from the mean spectrum, and the filled circles are based on the measurement of σ_{line} from the rms spectrum. The luminosity measurements have been corrected for the contribution from host galaxy starlight using the corrections of Bentz et al. (2006a). We have added the lowest luminosity data point described in this work to the set previously examined by Collin et al., but we use $\sigma_{blue,sym}$ from both the mean and rms spectra because of the blending issues discussed earlier in § 3.2.

Inspection of Figure 7 shows that the virial product for NGC 5548 is consistent with being independent of luminosity state.

This is as expected, since the black hole mass should not be varying with luminosity. The largest outlier is again from Year 12 (2000) of the AGN Watch program (Peterson et al. 2002).

Formal likelihood analysis of the black hole mass measurements gives a width of 0.15 dex, which is comparable to the standard deviation of the measurements themselves. From this we may conclude that the intrinsic scatter dominates the errors for repeated reverberation-based mass measurements of a single object.

While the reverberation-mapping experiment appears to be quite repeatable with a fairly high precision, we do not have an independent measurement of the systematic errors present in reverberation-mapping techniques. In order to estimate the systematic errors, we must compare results with a complementary method of measuring M_{BH}. Comparison of reverberation-mapping results to those derived from the M_{BH}-σ_* relationship shows that there is a factor of ~3 scatter in M_{BH} measurements from reverberation mapping (Onken et al. 2004). It is therefore important that inclination and other effects be considered in order to reduce the systematic errors in reverberation-mapping results.

5. CONCLUSIONS

We present the lowest luminosity ($L_{5100} = 4.7 \times 10^{42}$ ergs s^{-1}) monitoring data for NGC 5548. We measure a rest-frame time lag of $6.3^{+2.6}_{-2.3}$ days for changes in the Hβ line flux relative to changes in the continuum flux. Combining this new data point with previously collected data, we find the weighted mean of the black hole mass to be $M_{BH} = 6.54^{+0.26}_{-0.25} \times 10^7$ $M_\odot$.

With the results of this low-luminosity monitoring campaign, we are able to extend the range over which we may examine several relationships that depend on luminosity. We confirm the existence of a virial relationship between the time lag and the line width of the broad emission lines in NGC 5548. We find that the relationship between luminosity and time lag in NGC 5548 is consistent with a virial expectation, and is also consistent with the relationship determined for the entire population of AGNs with mass measurements from reverberation mapping.

REFERENCES

Bentz, M. C., Peterson, B. M., Pogge, R. W., Vestergaard, M., & Onken, C. A. 2006a, ApJ, 644, 133
Bentz, M. C., et al. 2006b, ApJ, 651, 775
Berezin, V. Y., et al. 1991, Soviet Astron. Lett., 17, 405
Blandford, R. D., & McKee, C. F. 1982, ApJ, 255, 419
Cackett, E. M., & Horne, K. 2006, MNRAS, 365, 1180
Collier, S., & Peterson, B. M. 2001, ApJ, 555, 775

Collin, S., Kawaguchi, T., Peterson, B. M., & Vestergaard, M. 2006, A&A, 456, 75
Denney, K., et al. 2006, ApJ, 653, 152
Edelson, R. A., & Krolik, J. H. 1988, ApJ, 333, 646
Ferrarese, L., Pogge, R. W., Peterson, B. M., Merritt, D., Wandel, A., & Joseph, C. L. 2001, ApJ, 555, L79
Gaskell, C. M., & Peterson, B. M. 1987, ApJS, 65, 1

Gaskell, C. M., & Sparke, L. S. 1986, ApJ, 305, 175
Horne, K., Welsh, W. F., & Peterson, B. M. 1991, ApJ, 367, L5
Hunt, L. K., Mannucci, F., Testi, L., Migliorini, S., Stanga, R. M., Baffa, C., Lisi, F., & Vanzi, L. 1998, AJ, 115, 2594
Kobayashi, Y., Yoshii, Y., Peterson, B. A., Minezaki, T., Enya, K., Suganuma, M., & Yamamuro, T. 1998a, in Proc. SPIE, 3354, 769
Kobayashi, Y., et al. 1998b, in Proc. SPIE, 3352, 120
Korista, K. T., & Goad, M. R. 2004, ApJ, 606, 749
Landolt, A. U. 1992, AJ, 104, 340
Onken, C. A., Ferrarese, L., Merritt, D., Peterson, B. M., Pogge, R. W., Vestergaard, M., & Wandel, A. 2004, ApJ, 615, 645
Peterson, B. M. 1993, PASP, 105, 247
Peterson, B. M., & Wandel, A. 1999, ApJ, 521, L95
Peterson, B. M., Wanders, I., Horne, K., Collier, S., Alexander, T., Kaspi, S., & Maoz, D. 1998, PASP, 110, 660

Peterson, B. M., et al. 1991, ApJ, 368, 119
———. 2002, ApJ, 581, 197
———. 2004, ApJ, 613, 682
———. 2005, ApJ, 632, 799
Storey, P. J., & Zeippen, C. J. 2000, MNRAS, 312, 813
Suganuma, M., et al. 2004, ApJ, 612, L113
Tremaine, S., et al. 2002, ApJ, 574, 740
van Groningen, E., & Wanders, I. 1992, PASP, 104, 700
White, R. J., & Peterson, B. M. 1994, PASP, 106, 879
Yoshii, Y. 2002, in New Trends in Theoretical and Observational Cosmology, ed. K. Sato & T. Shiromizu (Tokyo: Universal Academy), 235
Yoshii, Y., Kobayashi, Y., & Minezaki, T. 2003, BAAS, 202, 3803